



# Fatigue analysis of metallic-plastic-metallic pipeline systems: A numerical study

Ji-Sung Lee<sup>a,\*</sup>, Wei Zeng<sup>a</sup>, Martin Lambert<sup>b</sup>, Timothy Hilditch<sup>a</sup>, Jinzhe Gong<sup>a</sup>

<sup>a</sup> School of Engineering, Deakin University, Geelong Warrn Ponds Campus, Warrn Ponds, Victoria, 3216, Australia

<sup>b</sup> School of Civil, Environmental and Mining Engineering, University of Adelaide, SA 5005, Australia

## ARTICLE INFO

### Keywords:

Fatigue failure  
Fluid-structure interaction  
Pipe breaks  
Water hammer  
Pressurized pipe flow

## ABSTRACT

Metallic (e.g., copper, steel and iron) and plastic (e.g., Polyethylene and Polyvinyl chloride) pipelines are often used in combination in water distribution networks (WDSs). The interface between a metallic pipe section and a plastic pipe section is typically associated with a significant change in hydraulic impedance (i.e., impedance mismatch). This impedance mismatch can result in significant pressure wave reflections during transient events, and multiple interfaces may induce repeated pressure waves bouncing in between. Limited studies have been conducted on the impact of these multiple wave reflections due to impedance mismatch, especially with respect to the risk of accelerated fatigue damage to the plastic pipe. The research presented in this paper investigates the pressure response of a metallic-plastic-metallic (M-P-M) pipeline system under repeated hydraulic transient events using analytical and numerical methods. The presence of additional cyclic hoop-stress loadings in the M-P-M configuration, both in frequency due to reflections and in loading magnitude due to superposition, has been demonstrated in comparison to a fully plastic pipe system under the same hydraulic transient event. The study investigates the impact of these additional loadings on the relative fatigue lifetime of the plastic section by adopting a fatigue analysis model based on the stress-life method. The results show that the plastic section in the M-P-M configuration can have a significant reduction in fatigue lifetime compared to the corresponding fully plastic configuration.

## 1. Introduction

Pipe failure is one of the ongoing issues in the water industry, but it is difficult to predict pipe failure due to the increasing complexity in water distribution systems (WDSs). Many factors are involved in pipe failures such as internal and external loadings, material deterioration, or third-party interference [1]. One of the factors causing a pipe failure is the hydraulic transients in WDSs. Hydraulic transients commonly occur due to system operation (e.g., sudden valve closure, pump failure or hydrant operation) and maintenance [2–4]. The hydraulic transients have been widely used for leak detection or pipe condition assessment in the literature [5], however the effects of hydraulic transients on the risk of pipe failure have been studied for certain cases only such as failure of corrosion affected buried cast iron pipes [6], cast iron water network with pump connection [7] or high pressure deep gas well [8]. Large amplitude of transients or repeated transients over long periods can cause a catastrophic failure or fatigue failure of a pipe respectively [7].

Fatigue type failure has been emphasized in the field observation. Recent field studies have reported that the occurrence of various ranges of random pressure transients with fast repeating intervals [9]. Thus, it is important to understand the behaviour of the pressure transients to predict a pipe failure and it helps to mitigate the potential pipe failure by pipe system design with a proper understanding of pressure transients [10,11]. However, it is difficult to understand the behaviour of the pressure transients because WDSs often involve complex pipeline configurations and operational scenarios that were not originally designed to accommodate growing demands in an urban area [12,13].

One of the most common complex pipeline systems is a combination of metallic and plastic pipes in the network. Metallic pipes (such as cast and ductile iron pipes) have been widely used in WDSs for centuries, but their condition deteriorates over time due to factors such as pitting or corrosion [14]. When deteriorated metallic pipes are replaced, plastic pipes are often used instead of conventional metallic pipes. In the past two decades, plastic pipes such as High-Density Polyethylene (HDPE) and Polyvinyl Chloride (PVC) pipes have become increasingly popular in

\* Corresponding author.

E-mail addresses: [leejsu@deakin.edu.au](mailto:leejsu@deakin.edu.au) (J.-S. Lee), [w.zeng@deakin.edu.au](mailto:w.zeng@deakin.edu.au) (W. Zeng), [martin.lambert@adelaide.edu.au](mailto:martin.lambert@adelaide.edu.au) (M. Lambert), [tim.hilditch@deakin.edu.au](mailto:tim.hilditch@deakin.edu.au) (T. Hilditch), [james.gong@deakin.edu.au](mailto:james.gong@deakin.edu.au) (J. Gong).

<https://doi.org/10.1016/j.rineng.2023.100986>

Received 8 January 2023; Received in revised form 21 February 2023; Accepted 24 February 2023

Available online 27 February 2023

2590-1230/© 2023 The Authors. Published by Elsevier B.V. This is an open access article under the CC BY-NC-ND license (<http://creativecommons.org/licenses/by-nc-nd/4.0/>).

List of symbols			
$a$	Elastic wave speed (m/s)	$L^*$	Normalized pipe length ratio (–)
$A$	Cross-sectional area of pipe (m <sup>2</sup> )	$n_i$	Number of cycles per year (–)
$B = a/gA$	Hydraulic impedance	$N_R$	Number of the pressure variation cycles at considered value (–)
$B^*$	Impedance ratio between metallic and plastic pipe materials (–)	$P$	Internal pressure (kPa)
$D_0$	External diameter of pipe (m)	$p_i$	Pressure variation (kPa)
$D_i$	Internal diameter of pipe (m)	$Q_G$	Flow rate through side discharge (L/m <sup>3</sup> )
$e_{\min}$	Minimum thickness of pipe wall (m)	$Q_i$	Initial steady-state flow (L/m <sup>3</sup> )
$f$	Darcy-Weisbach friction factor (–)	$R = fQ_0/2D_iA$	Theoretical damping rate (–)
$FL$	Expected fatigue lifetime of pipe (–)	$SDR$	Standard diameter ratio (–)
$FL_{MPM}$	Expected fatigue lifetime of plastic pipe in M-P-M system (–)	$t_0$	Start time of the incident pulse wave (s)
$FL_P$	Expected fatigue lifetime of plastic pipe in fully plastic pipe system (–)	$T^*$	Normalized pulse duration (–)
$FL_R$	Relative fatigue lifetime (–)	$\Delta t_p$	Pulse duration (s)
$g$	Gravitational acceleration (m/s <sup>2</sup> )	$\sigma_{amp}$	Stress amplitude (kPa)
$H$	Pressure head (m)	$\sigma_{mean}$	Mean stress (kPa)
		$\sigma_{peak}$	Peak stress (kPa)
		$\sigma_{range}$	Stress range (kPa)
		$\sigma_h$	Hoop stress (kPa)

WDSs due to their lightweight and corrosion-resistant properties. As a result, many pipe systems now involve a combination of metallic and plastic pipe sections. One typical configuration is the metallic-plastic-metallic in series (M-P-M), in which a plastic pipe section is connected to metallic pipes at both ends. Other common configurations of metallic-plastic combined systems include metallic-plastic in series (M – P), where a plastic section is only connected to a metallic pipe at one end, and a plastic section connected to a metallic pipe as a branch.

One issue that must be considered in metallic-plastic combined systems is the complex pressure wave propagation and reflections. Some researchers have investigated wave propagation in these systems, but their focuses has typically been on pressure suppression due to an integrated plastic pipe section in a metallic pipe system. Pezzinga and Scandura [15] conducted an experimental study with additional polymeric pipes inserted at the upstream end of pipeline and observed that reductions of unsteady-flow oscillations. This research was extended in Pezzinga [16] using a quasi-2D model which illustrated the effects of the pressure suppression by inserting a branched polymeric pipe downstream of the pump in a pipe network. Gong et al. [17] conducted a field study on a M-P-M system, which demonstrated that the M-P-M configuration can help suppress pressure surges generated in the plastic section. Numerical and experimental studies also have been conducted using M-P-M configuration in Kubrak et al. [18], and it results that in-line plastic section into the steel pipeline system can suppress the pressure surges. Bettaieb et al. [19] used a branched network to investigate the transient response of three different configurations with various lengths and locations of plastic pipe sections as branches, and found that the low impedance of a pipe section can suppress the pressure in certain cases. Hadj Taieb et al. [20] used a complex pipeline system to analyse the effects of pressure suppression in a metallic-plastic combined system (the plastic pipe section is part of a branch in a branched network originally made of cast iron pipes) by assessing the structural integrity of cast iron (CI) pipes with semi-elliptical external defects. Combined technique (HDPE-LDPE) has been used in Triki and Chaker [21] to control surge pressure in a sensitive zone. The cited papers have demonstrated the damping effects of pressure wave due to the inserted plastic pipe in the metallic pipe, however, cyclic loading experienced in the plastic pipe due to reflected waves has not been addressed.

A potential negative effect of the metallic-plastic combined system that has not been addressed in the literature is the long-term impact from the additional pressure wave cycles under hydraulic transient events. The additional pressure wave cycles are due to the multiple wave

reflections at the interfaces between metallic and plastic pipe sections. The reflection of a pressure wave at the interface is governed by the impedance difference, which has been demonstrated in Chaudhry [22] and Gong et al. [17]. Since plastic pipes typically have a much lower wave speed than metallic pipes, the hydraulic impedance of plastic pipes is much lower than that of metallic pipes of the same diameter. When metallic and plastic sections are in mixed use, significant impedance mismatch exists, which can result in significant wave reflections.

Reflected pressure waves lead to additional cyclic pressure loadings on a plastic pipe, while multiple reflected pressure waves may be superimposed and undesirably accumulate pressure in the plastic pipe section when a transient is generated in a plastic section [21,23]. The pressure wave accumulation and additional cyclic stresses may accelerate fatigue failure in a plastic pipe section when compared to a fully plastic pipeline system; however, research on this topic is limited. A preliminary numerical case study was conducted by Lee et al. [24] on a M-P-M PVC pipeline system, where it was found that the fatigue lifetime of the plastic pipe section in the M-P-M configuration can be as low of 30% of that in the fully plastic configuration (under the specific hydraulic transient scenarios considered).

The research reported in this paper proposes a generalized model to predict the life expectancy of the plastic pipe section in M-P-M pipeline systems experiencing hydraulic transients. A stress-lifetime fatigue model proposed in Folkman and Bishop [25] was used as the basis to develop an analytical model to determine the resultant cyclic pressure loading due to multiple wave reflections in the plastic pipe section. Numerical simulations were conducted to validate the analytical model. Thereafter, a normalized fatigue analysis was conducted for M-P-M pipe systems using the stress-lifetime fatigue model to quantify the effect of the cyclic pressure loading. Practical issues related to real applications are briefly discussed before drawing conclusions. While previous researches have focused on the positive impact of M-P-M pipe system, the presented work raises awareness of negative impacts of the mixed use of metallic and plastic pipe sections. It can accelerate fatigue failure when compared to a fully plastic pipe configuration (which is used in standard pipe design).

## 2. Fatigue analysis models for pipelines

### 2.1. Background

Conventionally, uniform cyclic stress loading and a fully plastic pipe configuration are assumed for fatigue studies on plastic pipelines

[25–29]. In the fatigue studies of plastic pipelines, empirical models are normally used. Empirical fatigue analysis is typically conducted by one of two approaches: the stress-lifetime method [25–27,30,31] or the fracture mechanics-based method [32–35]. The stress-lifetime method uses an S–N diagram to represent the relationship between stress ( $S$ ) and the number of cycles to failure ( $N$ ). The S–N diagram is established by cyclic testing of pipe samples with a given stress range. One of the design guidelines for cyclic pressure in PVC pipes is presented in AWWA [36] based on a model presented in Jeffrey et al. [26]. Jeffrey et al. [26] summarized the results of previous studies [27,37,38]. However, it has been claimed by design engineers that this approach is confusing to many practitioners because the solution usually requires solving the roots of an equation. Another disadvantage of Jeffrey et al. [26]’s approach is its inaccuracy in the lower stress ranges (less than 400 psi). To simplify the analysis and avoid this problem at lower stress ranges, Folkman and Bishop [25] proposed a stress-lifetime fatigue model for PVC pipes using experimental fatigue data [26,30] with the effect from the mean stress neglected.

The fracture mechanics-based method is used when analysing pipes with small cracks. It directly analyses crack growth rates by modelling crack initiation and propagation [31]. Burn et al. [32] reviewed the fracture mechanics studies of PVC pipes and describes how to apply this method to predict fatigue failures. Important observation of these studies is that fatigue failures usually occur at the initiation site of a small flaw or defect. However, the significance of the initial defect is varied by size, shape, distribution, and location. Thus, the fracture mechanics method needs a stochastic model of the defect condition.

In both stress-lifetime method and fracture mechanics-based method, the predicted lifetime of a pipe is strongly dependent on number of cycles and magnitude of the applied stress range. However, most plastic pipeline fatigue studies are limited to uniform pressure loading and do not consider the impact of the dynamic stresses due to multiple reflections in an M-P-M pipeline system.

## 2.2. Stress-lifetime fatigue model

The stress-lifetime method proposed in Folkman and Bishop [25] is used in this research to facilitate fatigue analysis of M-P-M pipeline systems. To better illustrate the process, a general illustration of cyclic hoop stress and associated terms, including stress amplitude ( $\sigma_{amp}$ ),

mean stress ( $\sigma_{mean}$ ), peak stress ( $\sigma_{peak}$ ) and stress range ( $\sigma_{range}$ ) are defined as shown in Fig. 1.

Pipe failures often occur in cases where pipe walls are fatigued by stresses exerted upon them, and one of major components is hoop stress caused by internal water pressure. If pipes are installed properly, the hoop stress along radial direction will be dominant stress [25]. External constraints due to soil loads are small and can be neglected in a properly installed pipe. The effects of external constraints are neglected in this study. Relationship between hoop stress ( $\sigma_h$ ) and internal operating water pressure is given by Eq. (1).

$$\sigma_h = \frac{1}{2} P (SDR - 1) \quad (1)$$

where  $P$  represents internal pressure,  $SDR$  is standard diameter ratio ( $SDR = D_o/e_{min}$ ),  $D_o$  is external diameter of the pipe and  $e_{min}$  is minimum thickness of the pipe wall.  $P$  is gauged pressure when considering water pipes (i.e., absolute pressure – atmospheric pressure). In this research, only situations with positive  $P$  values are considered to ensure Eq. (1) is valid.

In this paper, the empirical model proposed by Folkman and Bishop [25] is used to investigate negative impacts of M-P-M system in WDSs. According to Folkman and Bishop [25], the fatigue life of the plastic pipe can be determined by Eq. (2).

$$FL = \frac{1.247E + 19}{(SDR - 1)^{4.006} \sum_{i=1}^{N_R} n_i \left( \frac{p_i}{6.895} \right)^{4.006}} \quad (2)$$

where  $FL$  is the expected life of pipe in years,  $p_i$  is the pressure range (difference between the maximum and minimum pressure) considered (in kPa) which represents pressure range ( $\sigma_{range}$ ) in Fig. 1,  $n_i$  is the number of cycles per year at pressure variation  $p_i$ , and  $N_R$  is the number of the pressure range ( $p_i$ ) considered. In this study, it is assumed that the experienced internal pressure is within yield stress of the pipe material to focus on the effect of repeated pressure waves on the pipe.

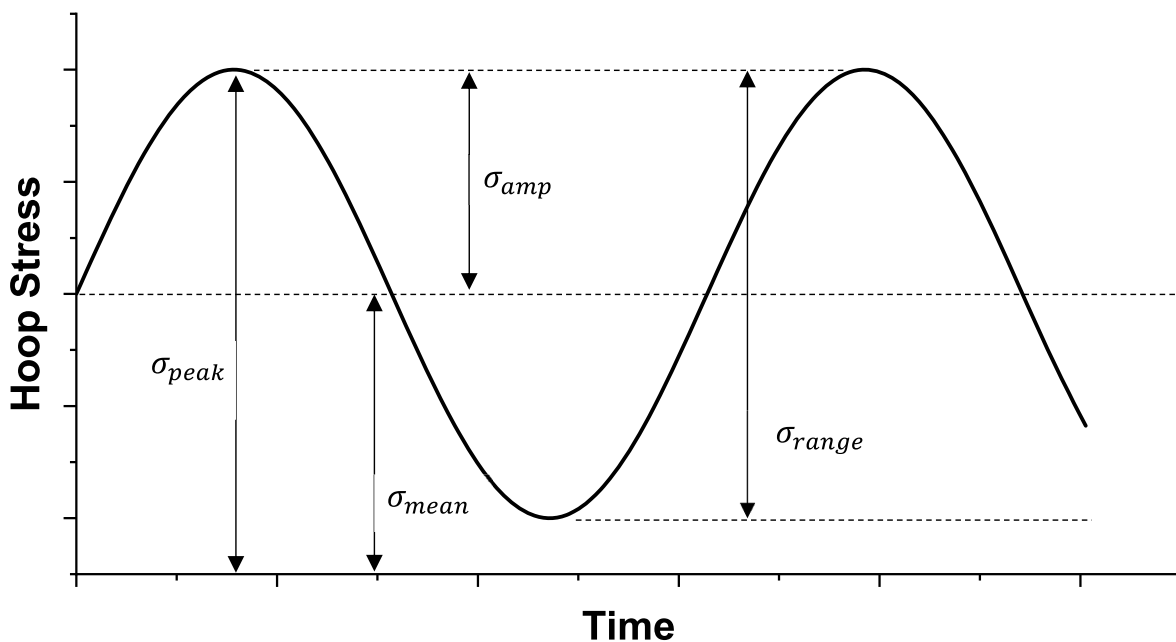


Fig. 1. The general form of stress history.

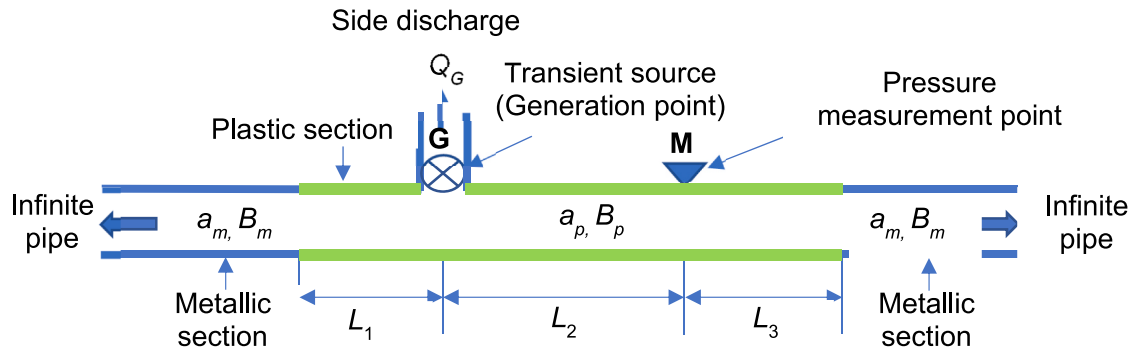


Fig. 2. Configuration of a metallic-plastic-metallic pipeline system.

### 3. Transient wave propagation analysis model

#### 3.1. System configuration

A general metallic-plastic-metallic (M-P-M) pipeline system as shown in Fig. 2 was used to investigate the pressure response under hydraulic transient events. The metallic sections are infinite in length, such that the effect of wave reflections at the metallic-plastic interfaces can be studied without interference from reflections at system boundaries. A fully plastic pipeline system having the same properties (i.e., pipe material, diameter and thickness) as the plastic section in the M-P-M system is used for comparison, and it is shown in Fig. 3.

The hydraulic pipeline impedance [22] is defined as

$$B = \frac{a}{gA} \quad (3)$$

where  $a$  is the elastic wave speed,  $g$  is the gravitational acceleration, and  $A$  is the cross-sectional area of the pipe. The wave speed and impedance for the plastic pipes are denoted as  $a_p$  and  $B_p$ , and  $a_m$  and  $B_m$  for the plastic and metallic pipe section respectively.

In the M-P-M system (Fig. 2), a side-discharge valve is placed at Point G, which is located at a distance of  $L_1$  from the left boundary of the plastic section. A pressure wave is generated by changing the side discharge  $Q_G$  (simulating water use by customers). Pressure is measured at M which is at a distance of  $L_3$  from the right boundary of the plastic section. The distance between the generation point (G) and the measurement point (M) is  $L_2$  and the total length of the plastic section is  $L$ . In the fully plastic pipe system (Fig. 3), the distance between the generation point and the measurement point is denoted as  $L_{G-M}$ . Note that the specific value of  $L_{G-M}$  has no effect on the results in the fully plastic system.

#### 3.2. Transient pressure wave excitation and reflections

In this research, negative pulse pressure waves will be generated and used for analysis. This is for ease of analysis using a stress-life fatigue model, and it does not lose generality since the focus is on comparing the M-P-M system (Fig. 2) with the fully plastic system (Fig. 3). Pulse shaped pressure waves are also common in real WDSs [17].

The side-discharge valve at Point G is assumed as closed at the initial stage. An incident pulse wave is generated by an opening valve just after time  $t_0$ , then closing the valve after time  $\Delta t_p$  (pulse duration). The initial head drop of the pulse wave ( $\Delta H_{G0}$ ) can be calculated by Eq. (4) based on the Joukowski surge pressure formula [39].

$$\Delta H_{G0} = B_p \frac{Q_G}{2} \quad (4)$$

where  $Q_G$  is the maximum flow rate through the side-discharge valve when the valve is opened.

To investigate the pulse wave analytically, a half-period cosine function waveform is used to generalise the incident pulse wave. Neglecting energy losses, pressure responses at the measurement point M at time  $t$  can be described as [17].

$$\Delta H_0(t) = \begin{cases} \frac{\Delta H_{G0}}{2} \left[ 1 - \cos\left(2\pi \frac{t - t_0}{\Delta t_p}\right) \right] & \text{for } t \in [t_0, t_0 + \Delta t_p] \\ 0 & \text{otherwise} \end{cases} \quad (5)$$

where  $t_0$  is the start time of the incident pulse wave and  $\Delta t_p$  is the pulse duration.

The incident pulse wave will propagate in two directions. Along the right direction, the incident wave will arrive at the measurement point M first and then be reflected at the right end of the plastic section due to the impedance mismatch at the boundary. Along the left direction, the incident wave will be reflected by the impedance mismatch at the left end of the plastic section and the reflected wave will reach point M. At

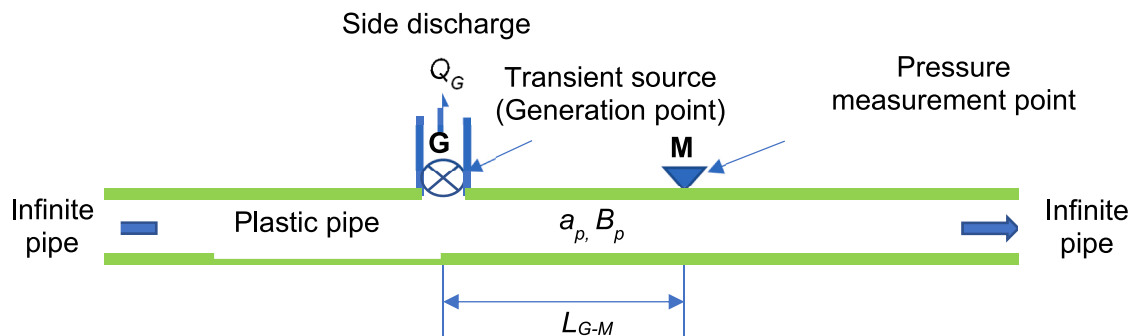


Fig. 3. Configuration of a fully plastic pipeline system.

**Table 1**  
Analytical equations for the incident wave and reflected waves.

Order	Wave path	Equation
1	G-M	$\Delta H_1(t) = \Delta H_0(t - \Delta t_2)$ (6)
2	G-Left-M	$\Delta H_2(t) = \left( \frac{1 - B_p/B_m}{1 + B_p/B_m} \right) \times \Delta H_0[t - (\Delta t_2 + \Delta t_1)]$ (7)
3	G-Right-M	$\Delta H_3(t) = \left( \frac{1 - B_p/B_m}{1 + B_p/B_m} \right) \times \Delta H_0[t - (\Delta t_2 + \Delta t_1 + \Delta t_3)]$ (8)
n		$\Delta H_n(t) = \left( \frac{1 - B_p/B_m}{1 + B_p/B_m} \right)^{\lfloor \frac{n}{2} \rfloor} \Delta H_0 \left( t - \lfloor \frac{n}{2} \rfloor \Delta t_1 - \lfloor \frac{n+1}{4} \rfloor \Delta t_3 - \lfloor \frac{n+1}{2} \rfloor \Delta t_2 \right)$ (9)

the boundaries between metallic and plastic pipes, where the impedance mismatch, the relative change in pressure head is related to the relative change in hydraulic impedance between two difference materials [17, 22,40]. Such wave propagation and reflection process will continue until the magnitude of the wave approaches zero. The sequence, wave paths and analytical equations of the incident wave and reflected waves are summarized in Table 1 with an assumption of  $L_3 > L_1$ . Note that only the order of the wave arrivals will change if  $L_3 < L_1$ , while the wave paths and theoretical equations for each wave are the same. For the purpose of fatigue analysis, the theoretical analyses for these two situations will be the same.

In Table 1,  $\Delta t_1 = 2L_1/a_p$ ,  $\Delta t_2 = L_2/a_p$  and  $\Delta t_3 = (2L_3 - 2L_1)/a_p$ . The symbol  $\lfloor \cdot \rfloor$  represents the floor function. Left and Right represent the left and the right end of the plastic section respectively. The magnitude of the first arriving wave will be the same as the Joukowski surge pressure obtained from Eq. (4). The second pressure wave (reflected by the left end of the plastic section) and third pressure wave (reflected by the right end of the plastic section) at the measurement point *M* can be described as Eqs. (7) and (8) respectively. They have the same pressure magnitude.

In the pulse wave analysis, there are two types of pulses that can be defined based on the pulse duration. For “short-duration pulses”, the duration of incident pulse ( $\Delta t_p$ ) is shorter than the minimum time gap between two adjacent pulses (i.e.,  $\Delta t_p < \min [\Delta t_1, \Delta t_2, \Delta t_3]$ ). In this case, these pressure waves are not superimposed. If  $\Delta t_p > \min [\Delta t_1, \Delta t_2, \Delta t_3]$ , it can be defined as “long-duration pulses”. Some pressure waves will be superimposed in this case [17] because the following reflected waves are arrived at the measurement point before the end of first wave. In the fully plastic pipe configuration (Fig. 3), there is no wave reflections, and the original incident pulse wave is the only wave to consider. Pressure accumulation in M-P-M system is highly dependent on the time interval between arrived pressures ( $\Delta t_1, \Delta t_2, \Delta t_3$ ) and pulse duration ( $\Delta t_p$ ), thus, severe pressure accumulation could be developed if the replaced plastic section is shorter when the pulse duration is same [23].

Under the linear system theory, the pressure responses at measurement point *M* can be described as a superposition of all the sequence of pulse perturbations regardless of the pulse duration, and it can be described as

$$\Delta H(t) = \sum_{n=1}^{\infty} \Delta H_n(t) \quad (10)$$

By substituting the analytical wave equations in Table 1 into Eq. (10), Eq. (11) can be derived to describe the overall pressure response at the measurement point *M* as a function of time related to the given pulse duration  $\Delta t_p$ .

$$\Delta H(t^*) = \sum_{n=1}^{\infty} \left( \frac{1 - \frac{B_p}{B_m}}{1 + \frac{B_p}{B_m}} \right)^{\lfloor \frac{n}{2} \rfloor} \times \frac{H_{G0}}{2} [1 - \cos(2\pi(t^* - t_n^*))] \quad (11)$$

where  $t^* = t/\Delta t_p$  and  $t_n^* = [(1 + 2\lfloor \frac{n-1}{4} \rfloor)\Delta t_2 - \lfloor \frac{n}{2} \rfloor \Delta t_1 - \lfloor \frac{n+1}{4} \rfloor \Delta t_3] / \Delta t_p$ .

Equation (11) allows analysing the pressure responses in M-P-M pipeline systems with a lossless assumption. This helps to calculate the pressure responses for various pulse scenarios and pipe configurations without conducting a numerical simulation. For fatigue analysis, it can be used to calculate the estimated fatigue life of the plastic pipe in the M-P-M pipeline system.

### 3.3. Effects of energy losses

In the previous section, energy losses are not considered in the analysis. However, energy losses in real plastic pipes will induce damping to the pressure waves, which reduces the stress loading experienced on the pipe wall. Energy losses can be caused by many factors such as fluid-structure interaction (FSI) [41], viscoelasticity [42,43] and steady and unsteady friction [22,44].

In this study, to capture the effect of energy losses (damping) on the fatigue life of plastic pipes, a concept of damping rate, *R*, is introduced. The damping rate concept has been introduced to reflect the energy loss effects (which cannot be avoidable in real system) in fatigue lifetime analysis, it creates proportional energy loss effects on pressure response in the analysis. The damping rate (*R*) represents wave dissipation caused by steady friction with Darcy-Weisbach friction factor. When only steady friction is considered, the theoretical damping rate can be calculated by [45].

$$R = \frac{fQ_0}{2D_iA} \quad (12)$$

where *f* = Darcy-Weisbach friction factor,  $Q_0$  = initial steady-state flow, and  $D_i$  = internal diameter of the pipe.

Considering the damping rate *R*, Eq. (11) can be modified as

$$\Delta H_e(t) = \sum_{n=1}^{\infty} \left( \frac{1 - \frac{B_p}{B_m}}{1 + \frac{B_p}{B_m}} \right)^{\lfloor \frac{n}{2} \rfloor} \times \frac{H_{G0} \times e^{-Rt}}{2} [1 - \cos(2\pi(t^* - t_n^*))] \quad (13)$$

In the numerical studies discussed later, the damping rate *R* (based on Darcy-Weisbach friction factor) will be used as a lumped term to



**Table 2**  
Specifications of the pipelines in the Numerical Simulations.

Specification	Case 1		Case 2	
	PVC-O DN225	DI DN200	PVC-O DN150	DI DN200
Internal diameter, $D_i$ (mm)	234.2	200	160.1	200
Outside diameter, $D_o$ (mm)	258.9	232	177.6	232
Wall thickness, $e$ (mm)	12.6	5	8.7	5
Elastic modulus, $E_0$ (GPa)	2.8	170	2.8	170
Poisson's ratio	0.38	0.3	0.38	0.3
Constraint factor, $c$	0.961	0.953	0.961	0.953
Elastic wave speed, $a$ (m/s)	367.4	1157.2	369.3	1157.2
Impedance, $B$ (s/m <sup>2</sup> )	869	3755	1870	3755
Length				
$L_1$ , (m)	25			
$L_2$ , (m)	50			
$L_3$ , (m)	25			
Flow through side valve, $Q_G$ (m <sup>3</sup> /s)	0.02			

represent all energy losses. In this study, large values of  $R$  have been assigned intentionally to represent other factors such as FSI, viscoelasticity and unsteady friction in general.

#### 4. Numerical simulation

Numerical case studies have been conducted to verify the findings described in the previous sections. The method of characteristics (MOC) [39] has been used to simulate pressure responses in pipeline systems. Cases have been designed based on practical cases in real pipeline systems [9] that incorporates PVC and ductile iron (DI) pipe sections.

The system configurations used in this numerical case are based on those shown in Figs. 2 and 3. The specifications used in the various cases are summarized in Table 2. The boundary condition of both pipeline systems is assumed to be infinitely long to avoid boundary reflections, and it will highlight the impact of the impedance mismatch. Pipes in both configurations are assumed to be constrained throughout. The pressure at the upstream and downstream ends of the pipe systems are both 60 m and remain constant. The time step used in the MOC model is 0.001 s. The number reaches after discretization for section  $L_1$ ,  $L_2$  and  $L_3$  are 68, 136 and 68, respectively. Pulse pressure waves are simulated by initiating a peak side discharge of  $Q_G$  and then stopping it. Total length ( $L$ ) of plastic pipe is 100 m. The length of plastic pipe sections ( $L_1$ ,  $L_2$  and  $L_3$ ) are 25 m, 50 m and 25 m respectively. Series of numerical cases have been conducted with different pulse durations, magnitudes of the incident pressure wave, diameters of the pipe, and lengths of the plastic pipe.

To simplify the analysis, it is assumed that  $L_1 = L_3$  in the numerical simulations. When  $L_1 = L_3$ , it implicates the most critical scenario. Because the second and third pulse waves are superimposed by the system configuration, thus it increases the risk of fatigue acceleration [24]. The total length of plastic pipe section is 100 m for ease of analysis. The length of replaced section with plastic pipe can vary from a few meters to a few hundred meters in the field [46]. The pressure responses are calculated by the theoretical analysis (Eq. (11)) and the numerical simulation (MOC).

##### 4.1. Fatigue analysis without energy loss

In this section, fatigue analysis is conducted without considering energy loss. The cases considering energy loss will be conducted in the next section and will be compared with the cases without considering energy loss. The effects of energy loss will be discussed in the next section.

The analysis is conducted using two cases presented in Table 2. By using two different diameters of plastic pipe (the diameter of the metallic pipe is the same for both cases), the effects of different impedance ratios can be investigated. Since the minimum of  $[\Delta t_1, \Delta t_2, \Delta t_3]$  is 0.216 s, two pulse pressure waves with a duration of 0.1 s (short-duration pulse) and 1 s (long-duration pulse), respectively, are considered.

Fig. 4 shows the numerical results of the transient pressure responses of Case 1 subject to pulse waves. For the M-P-M pipeline system as shown in Fig. 4(a), the magnitude values of the first pulse wave with  $\Delta t_p$

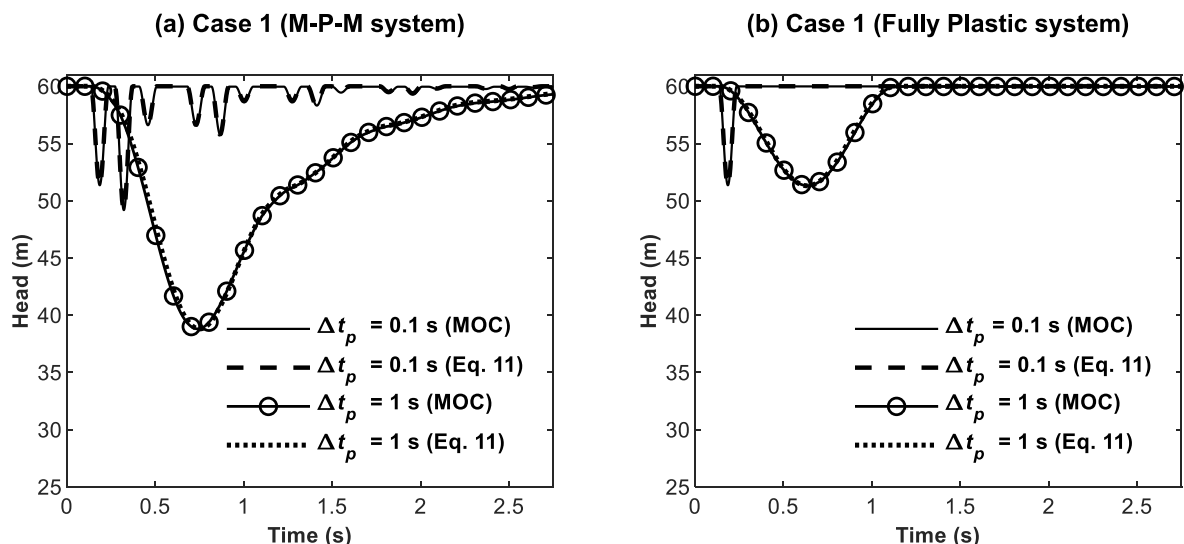


**Fig. 4.** Pressure responses of Case 1 for the M-P-M and the Fully Plastic systems using Eq. (11) and numerical simulation (MOC).

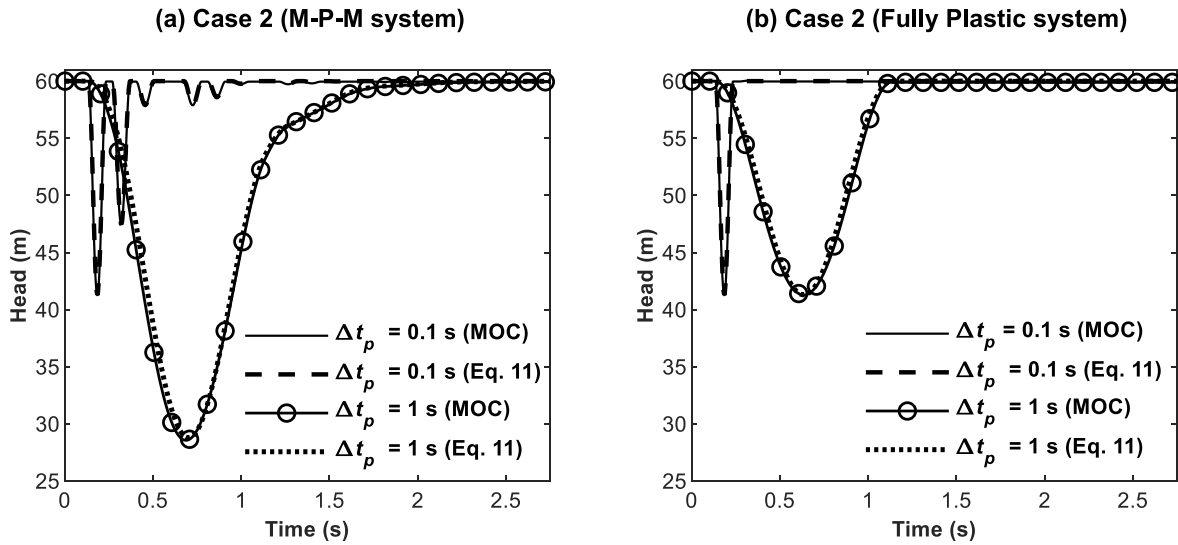


Fig. 5. Pressure responses of Case 2 for the M-P-M and the Fully Plastic systems using Eq. (11) and numerical simulation (MOC).

Table 3

The results of relative fatigue life from numerical simulation and analytical calculation (Eq. (11)).

	Case 1		Case 2	
	$\Delta t_p = 0.1$ s	$\Delta t_p = 1$ s	$\Delta t_p = 0.1$ s	$\Delta t_p = 1$ s
MOC Simulation	0.282	0.0280	0.842	0.124
Analytical [Eq. (11)]	0.283	0.0281	0.832	0.128

= 0.1 s is 8.69 m, which is consistent with the Joukowski equation (4). The second pulse wave with  $\Delta t_p = 0.1$  s is 10.85 m, which are consistent with the theoretical calculation from Eq. (11). As from a short-duration pulse excitation ( $\Delta t_p = 0.1$  s), the first pulse wave observed is the initial incident wave. When a long-duration pulse ( $\Delta t_p = 1$  s) is induced in the M-P-M pipeline system, wave superposition can be observed as shown in Fig. 4(a). The magnitude of the superimposed wave is 21.19 m, which is consistent with the theoretical calculation from Eq. (11). Comparing to the short-duration pulse, the long-duration pulse has increased the magnitude of the largest wave from 10.85 m to 21.19 m in Case 1. For the all-plastic pipeline system as shown in Fig. 4(b), the magnitude values of the pulse wave with different pulse durations are both 8.69 m.

Fig. 5 shows the numerical results of the transient pressure responses of Case 2 subject to pulse waves. For the M-P-M pipeline system as shown in Fig. 5(a), the magnitude values of the first and second pulse waves with  $\Delta t_p = 0.1$  s are 18.70 m and 12.53 m. The magnitude of the first pulse wave (the incident wave) is larger than the first pulse wave in Case 1. This is caused by a higher hydraulic impedance of plastic pipe in Case 2 ( $B_p = 869$  and 1870 for Case 1 and Case 2, respectively). According to the Joukowski equation, the higher hydraulic impedance creates a higher initial head perturbation (when the flow condition is the same). For the case with the long-duration pulse, the magnitude of the superimposed wave is 31.43 m. As a result of wave superposition, the magnitude of the maximum wave is increased from 18.70 m to 31.43 m in Case 2.

The pressure variations ( $p_i$ ) from the obtained pressure responses are calculated, and they are directly used in the fatigue model using Eqs. (1) and (2). The results of the relative fatigue life obtained from the pressure responses by the numerical simulation and analytical calculation (Eq. (11)) are presented in Table 3. Note that the numerical simulation results are consistent with the theoretical analysis (the range of difference between the two results is from 0.36 to 3.8%), which validates the theoretical analysis.

It can be found that the expected fatigue life of the plastic pipe in the M-P-M pipeline system is significantly lower than the case of the fully

plastic pipeline system. The expected lifetime of plastic pipe in the M-P-M system is 28.2% or 84.2% of the fully plastic pipe system when  $\Delta t_p = 0.1$  s. It can be significantly reduced with longer pulse duration. When a long-duration pulse ( $\Delta t_p = 1$  s) is induced in the system, the expected life of the plastic section in the M-P-M system for two cases is only 2.8% or 12.4% of the life of the corresponding fully plastic pipe case. These results provide further support for the findings that the impedance mismatch and multi-reflections may cause a significant life reduction in plastic pipes in metallic-plastic combined systems.

#### 4.2. Fatigue analysis with energy loss

In the previous section, the negative impacts of impedance mismatch have been demonstrated by neglecting the energy loss. To investigate the effect of energy loss on the relative fatigue lifetime, a simple steady friction model considered first to establish a benchmark. The Darcy-Weisbach friction factors were selected as  $f = 0.02$ , resulting in  $R = 0.0198$  and 0.0621 for Case 1 and Case 2, respectively. To consider energy loss contributors extended analyses have been conducted with much higher  $R$  values (0.5 and 1). If only friction loss is considered as the major contribution to  $R$ , factors like biofilm attached to the wall, pipe deterioration and flow rate will affect the  $R$  values. Fatigue analysis with energy losses is then conducted using Case 1 and Case 2 (Table 2).

Fig. 6 shows the pressure responses of Case 1 for the M-P-M with  $\Delta t_p = 0.1$  s and 1 s. The magnitude of the largest pulse wave from MOC simulations for  $R = 0.0198$  are 8.66 m and 21.0 m for  $\Delta t_p = 0.1$  s and 1 s, respectively, which are consistent with the theoretical calculation using Eq. (13). The magnitude is reduced distinctively for both cases when  $R$  is larger (e.g.,  $R = 0.5$  and 1).

Fig. 7 shows the pressure responses of Case 2 for the M-P-M subject to a 0.1 s and a 1 s pulse duration. The magnitudes of the largest pulse wave in the M-P-M system from MOC simulations are 18.5 m and 29.9 m for 0.1s and 1 s of pulse duration when the damping rate  $R$  is 0.0621. The results are consistent with the analytical calculations using Eq. (13). Further magnitude decrease can be observed when  $R$  is larger.

With the results of the pressure responses incorporating energy losses, the relative fatigue lifetimes ( $FL_R$ ) are calculated as shown in Table 4. The relative fatigue lifetime with a typical steady friction factor assumed ( $f = 0.02$ ) is very similar to the case without considering energy loss (Table 3). When a higher damping rate is applied, more discrepancies can be observed. However, the results still show significant decreases in the relative fatigue life compared with the fully plastic pipe.

The hydraulic pressure wave is damped per travelled length through

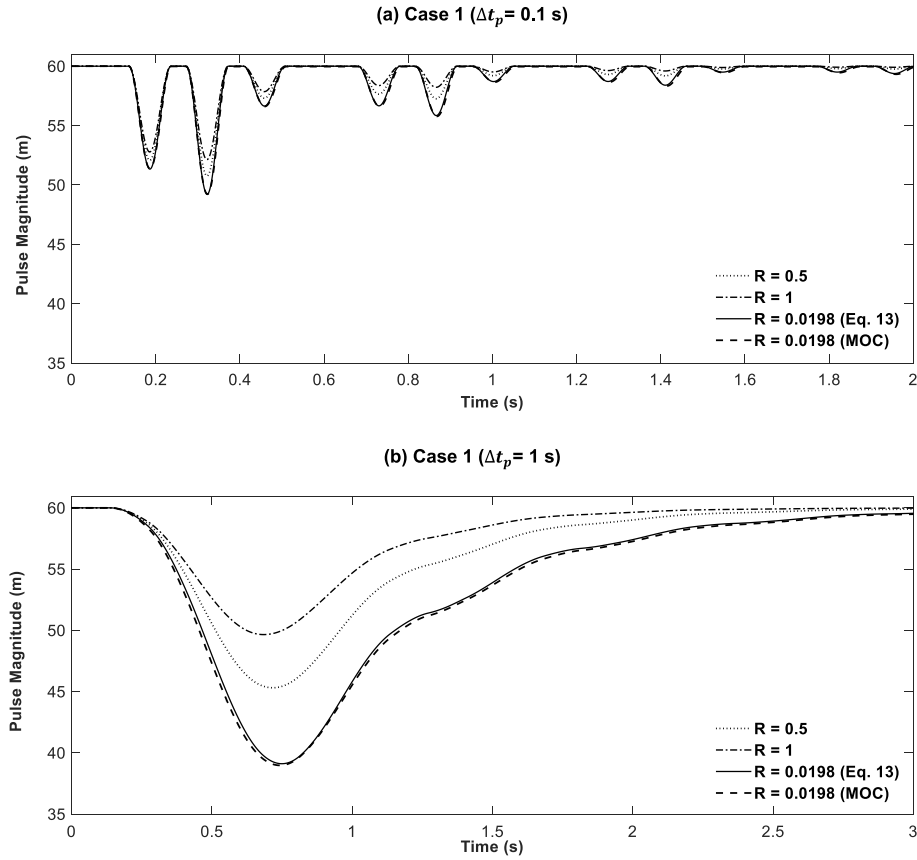


Fig. 6. Pressure responses of Case 1 for the M-P-M subject to (a) 0.1 s and (b) 1 s of pulse duration with frictional loss ( $R = 0.0621, 0.5$  and  $1$ ).

the pipe, and its impact is greater when the length of the plastic pipe is longer. To investigate the sensitivity of damping effects to the length of plastic pipe section in the M-P-M system (in Fig. 2), several lengths of plastic pipe ( $L = 1, 5, 10, 25, 50$  and  $100$  m) and attenuation values ( $R = 0.02, 0.5$  and  $1$ ) are analysed by numerical calculation only using Case 1. The normalized pulse duration ( $T^*$ ) is fixed as  $0.2$  to highlight the impact from the pipe length. The results of the relative fatigue life are presented in Fig. 8.

When the length of the plastic pipe is  $100$  m, the wave damping can cause a significant change (differences are from  $1.22\%$  to  $77.8\%$ ); however, the difference between the results with damping and without damping decreases as the length of the plastic pipe decreases. With the length reduced to less than  $5$  m, the difference becomes less than  $5\%$  even for the highest damping rate  $R = 1$ .

Energy losses can attenuate pressure waves and change relative fatigue lifetimes; however, the amount of wave damping would be similar to both M-P-M and the fully plastic pipeline systems. As a result, the finding of reduced expected fatigue lifetimes in M-P-M systems (relative to the fully plastic systems) is still valid even when the energy losses are considered.

## 5. Normalized fatigue analysis

In this section, a normalized analysis is conducted to derive a generalized equation applicable to M-P-M systems. Incident pulse waves are generated at the side-discharge valve (Point G).

The results of the numerical analysis in the previous section showed that the effects of energy losses are small (less than  $5\%$  even if the damping rate is significantly large) when the plastic pipe section is short in the M-P-M pipeline system. In the field, the damaged metallic pipe can

be cut out generally short in length and replaced by plastic pipe [46]. Thus, energy losses are neglected in this section considering that the plastic section in a M-P-M system is generally short. This also helps to focus on the impact of impedance mismatch on the fatigue life reduction. A relative lifetime ( $FL_R$ ) of a plastic pipe is defined by the ratio between the lifetime of the plastic pipe in the M-P-M configuration and that of the fully plastic pipe configuration.

To determine the relative lifetime of the plastic pipe ( $FL_R$ ), the range of the pressure variations needs to be determined from the pressure responses in both the M-P-M and the fully plastic pipeline systems. For cyclic stress loading, the difference between each local maximum point and the adjacent minimum point is defined as the stress range (Fig. 1). These maximum and minimum points in the pressure variation trace can be found by calculating the derivatives.

To obtain the corresponding time for a local maximum or minimum point, the first and second derivatives were calculated (the local maximum can be defined when  $f'(x) = 0$  and  $f''(x) < 0$ , and the local minimum can be defined when  $f'(x) = 0$  and  $f''(x) > 0$ ).

$$f'(t^*) = \sum_{n=1}^{\infty} \left( \frac{1 - \frac{B_p}{B_m}}{1 - \frac{B_p}{B_m}} \right)^{\left[ \frac{q}{2} \right]} \times \frac{H_{i0} \times \pi}{\Delta t_p} [\sin(2\pi(t^* - t_n^*))] \quad \text{for } t^* \in [0, 1] \quad (14)$$

$$f''(t^*) = \sum_{n=1}^{\infty} \left( \frac{1 - \frac{B_p}{B_m}}{1 - \frac{B_p}{B_m}} \right)^{\left[ \frac{q}{2} \right]} \times \frac{H_{i0} \times 2\pi^2}{\Delta t_p^2} [\cos(2\pi(t^* - t_n^*))] \quad \text{for } t^* \in [0, 1] \quad (15)$$



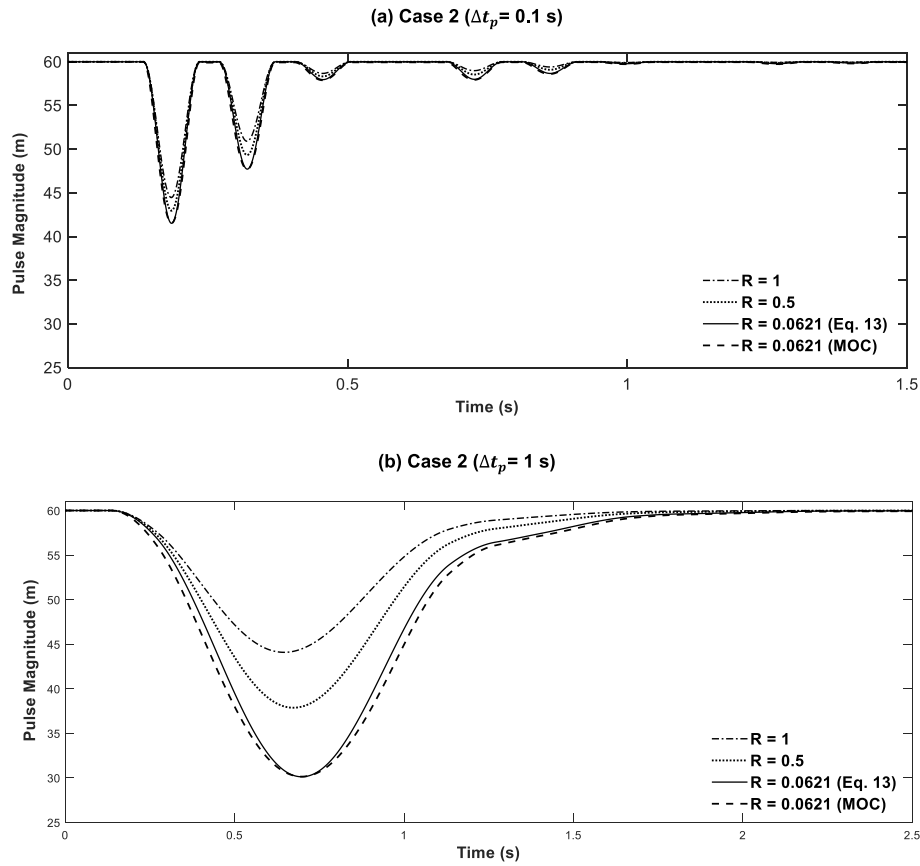


Fig. 7. Pressure responses of Case 2 for the M-P-M subject to (a) 0.1 s and (b) 1 s of pulse duration with frictional loss ( $R = 0.0621, 0.5$  and  $1$ ).

Table 4

The results of relative fatigue life ( $FL_R$ ) from numerical simulation and analytical calculation with consideration of energy loss.

		$\Delta t_p = 0.1$ s	$\Delta t_p = 1$ s
Case 1	$R = 0$ – Theoretical Analysis (Eq. (11))	0.283	0.0281
	$R = 0.0198$ ( $f = 0.02$ ) – MOC Simulation	0.283	0.0282
	$R = 0.0198$ ( $f = 0.02$ ) – Theoretical Analysis (Eq. (13))	0.286	0.0288
	$R = 0.5$ – Theoretical Analysis (Eq. (13))	0.347	0.0352
Case 2	$R = 1$ – Theoretical Analysis (Eq. (13))	0.413	0.0431
	$R = 0$ – Theoretical Analysis (Eq. (11))	0.832	0.129
	$R = 0.0621$ ( $f = 0.02$ ) – MOC Simulation	0.832	0.132
	$R = 0.0621$ ( $f = 0.02$ ) – Theoretical Analysis (Eq. (13))	0.837	0.131
	$R = 0.5$ – Theoretical Analysis (Eq. (13))	0.867	0.146
	$R = 1$ – Theoretical Analysis (Eq. (13))	0.895	0.166

From the derivatives, the specific time  $[t_{max}^*, t_{min}^*]$  corresponding to the local maximum and minimum points can be determined when

$$f'(t) = 0, t = \begin{cases} t_{min}^* & f''(t) > 0 \\ t_{max}^* & f''(t) < 0 \end{cases}.$$

$$t_{min}^* = [t_{min,1}^*, t_{min,2}^*, t_{min,3}^*, \dots, t_{min,i}^*] \quad (16)$$

$$t_{max}^* = [t_{max,1}^*, t_{max,2}^*, t_{max,3}^*, \dots, t_{max,i}^*] \quad (17)$$

By substituting Eq. (16) and Eq. (17) into Eq. (11), the magnitude of local maximum and minimum pressures can be calculated as

$$p_{min,i}(t_{min,i}^*) = \sum_{n=1}^{\infty} \left( \frac{1 - \frac{B_p}{B_m}}{1 - \frac{B_p}{B_m}} \right)^{\left| \frac{t_{min,i}^*}{\Delta t_p} \right|} \times \frac{1}{2} [1 - \cos(2\pi(t_{min,i}^* - t_n^*))] \quad (18)$$

$$p_{max,i}(t_{max,i}^*) = \sum_{n=1}^{\infty} \left( \frac{1 - \frac{B_p}{B_m}}{1 - \frac{B_p}{B_m}} \right)^{\left| \frac{t_{max,i}^*}{\Delta t_p} \right|} \times \frac{1}{2} [1 - \cos(2\pi(t_{max,i}^* - t_n^*))] \quad (19)$$

The stress range ( $p_i$ ) of each individual pressure variation can be then denoted as

$$p_i = (p_{max,i} - p_{min,i}) \quad (20)$$

By substituting the determined stress range ( $p_i$ ) into Eq. (2), the expected fatigue life for a plastic pipe can be then calculated. The relative fatigue life can be obtained by dividing the expected fatigue life of plastic pipe in the M-P-M system by the expected fatigue life of the fully plastic pipe system under the same hydraulic transient event, and thus

$$FL_R = \frac{FL_{MPM}}{FL_p} = \frac{\frac{1.247 \times 10^{19}}{(DR-1)^{4.006} \times 1.42197 \times n \times (H_{G0})^{4.006} \sum_{i=1}^N \frac{p_i^{4.006}}{6.895}}}{\frac{1.247 \times 10^{19}}{(DR-1)^{4.006} \times 1.42197 \times n \times (H_{G0})^{4.006} \sum_{i=1}^N \frac{p_i^{4.006}}{6.895}}} = \frac{1}{\sum_{i=1}^N \frac{p_i^{4.006}}{6.895}} \quad (21)$$

where  $FL_{MPM}$  is the expected fatigue life of plastic pipe in the M-P-M system and  $FL_p$  is the expected fatigue life of the fully plastic pipe system.

The relative fatigue life ( $FL_R$ ) of the plastic section in the M-P-M pipeline system represents a proportional fatigue life to the corresponding the fully plastic pipeline system with the same hydraulic

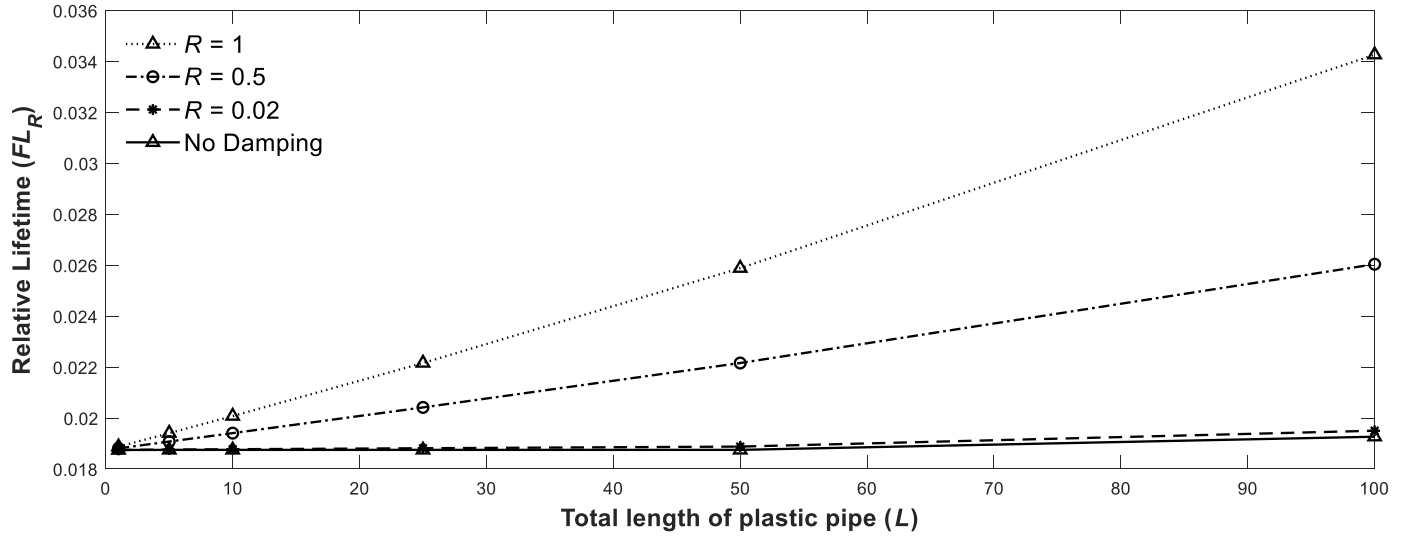


Fig. 8. The relative fatigue life of various lengths of the plastic pipe section for Case 1.

condition.  $FL_R$  shows that it is dependent on three parameters which are the impedance ratio between metallic and plastic materials ( $B^* = B_p/B_m$ ), the normalized pulse duration ( $T^* = T/t_p$ ), where  $T = L/a_p$ , and the normalized pipe length ratio which is defined as  $L^* = L_2/L$ . The impedance ratio ranges from 0 to 1, the normalized length ( $L^* = L_2/L$ ) ranges from 0 to 1 and the normalized pulse duration ( $T/t_p$ ) ranges from 0 to 4 in this study. As defined in the earlier section, the normalized pulse duration related to the wave travelling time in the plastic section can be described as  $t_n^*$  [as in Eq. (11)] and  $\Delta t_1^* = \frac{\Delta t_1}{t_p}$ ,  $\Delta t_2^* = \frac{\Delta t_2}{t_p}$ .

To simplify the analysis, it is assumed that  $L_1 = L_3$  in this section and  $t_n^*$  can be simplified as

$$t_n^* = \left(1 + 2 \left\lfloor \frac{n-1}{4} \right\rfloor\right) \Delta t_2^* - \left\lfloor \frac{n}{2} \right\rfloor \Delta t_1^* \quad (22)$$

The relationship between  $\Delta t_1^*$  and  $\Delta t_2^*$  is

$$\Delta t_1^* = T^* - \Delta t_2^* \quad (23)$$

$$\Delta t_2^* = \frac{L_2}{a_p \times t_p} = \frac{L_2}{L} \times \frac{L}{t_p \times a_p} = L^* \times T^* \quad (24)$$

Based on Eqs. (23) and (24), when  $L^* (= L_2/L)$  is determined,  $\Delta t_1^*$  and  $\Delta t_2^*$  can be described by  $L^*$  and  $T^* (= T/t_p)$ . By substituting the three normalized parameters into equations (18) and (19), the local minimum and maximum pressures can be described as below:

To understand the impacts of pulse duration, different normalized pulse durations from 0 to 4 are investigated. The higher normalized pulse duration (maximum  $T^* = 4$ ) indicates a short pulse duration, while the lower  $T^*$  (minimum  $T^* = 0.01$ ) indicates a large pulse duration. If the  $T^*$  is the minimum, the magnitude of the pulse reaches the maximum by head accumulation.

In the analytical pressure response (Eq. (11)), the “short-duration pulses” are defined as  $t_p < \min [\Delta t_1 (= \Delta t_3), \Delta t_2]$ . By using the relationship between  $\Delta t_1^*$  and  $\Delta t_2^*$  [in Eqs. (23) and (24)], the “short-duration pulses” in the normalized equation can be defined for two different cases.

When  $L^* < 1/3$  (in this case,  $L_2$  is smaller than  $L_1$  and  $L_3$ ), the threshold for “short-duration pulses” is  $L^* \times T^* (= \Delta t_2^*) > 1$ . If  $L^* \times T^* (= \Delta t_2^*) < 1$ , it can be defined as “long-duration pulses”. When  $> 1/3$  (in this case,  $L_2$  is larger than  $L_1$  and  $L_3$ ), the threshold for “short-duration pulses” is  $(1 - L^*)T^* > 1$ . If  $(1 - L^*)T^* < 1$ , it can be defined as “long-duration pulses”.

From the results in Fig. 9, several important findings can be summarized as follows.

- The relative fatigue life ( $FL_R$ ) ranges from 0 to 1. When  $FL_R = 1$ , it represents that the plastic section in the M-P-M configuration has an equivalent expected lifetime as the fully plastic pipe configuration.
- The fatigue life of the plastic section in the M-P-M configuration is decreased due to the reflected waves and the effect of wave superposition.

$$p_{min,i}(t_{min,i}^*) = \sum_{n=1}^{\infty} \left( \frac{1-B^*}{1+B^*} \right)^{\left\lfloor \frac{n}{2} \right\rfloor} \times \frac{1}{2} \left[ 1 - \cos \left( 2\pi \left( t_{min,i}^* - \left( 1 + 2 \left\lfloor \frac{n-1}{4} \right\rfloor \right) (L^* \times T^*) - \left\lfloor \frac{n}{2} \right\rfloor T^* (1 - L^*) \right) \right) \right] \quad (25)$$

$$p_{max,i}(t_{max,i}^*) = \sum_{n=1}^{\infty} \left( \frac{1-B^*}{1+B^*} \right)^{\left\lfloor \frac{n}{2} \right\rfloor} \times \frac{1}{2} \left[ 1 - \cos \left( 2\pi \left( t_{max,i}^* - \left( 1 + 2 \left\lfloor \frac{n-1}{4} \right\rfloor \right) (L^* \times T^*) - \left\lfloor \frac{n}{2} \right\rfloor T^* (1 - L^*) \right) \right) \right] \quad (26)$$

By substituting Eqs. (25) and (26) into Eqs. (20) and (21), the normalized fatigue life can be calculated and it is determined by three normalized parameters ( $L^*$ ,  $T^*$  and  $B^*$ ). When  $L^* = 0$ , it means that the generation and measurement points are both located in the middle of the plastic pipe in the M-P-M system. If  $L^* = 1$ , it indicates that the generation and measurement points are located at each end of the plastic pipe.

- When  $B^* = 1$ , the pipeline system is equivalent to a uniform pipeline system (e.g., a fully plastic pipeline system); therefore, the relative fatigue lifetime is always 1.
- If it is assumed that the case of the “short-duration pulses”, separated impulse wave responses are observed and thus the fatigue life is determined by the number and size of each individual wave.

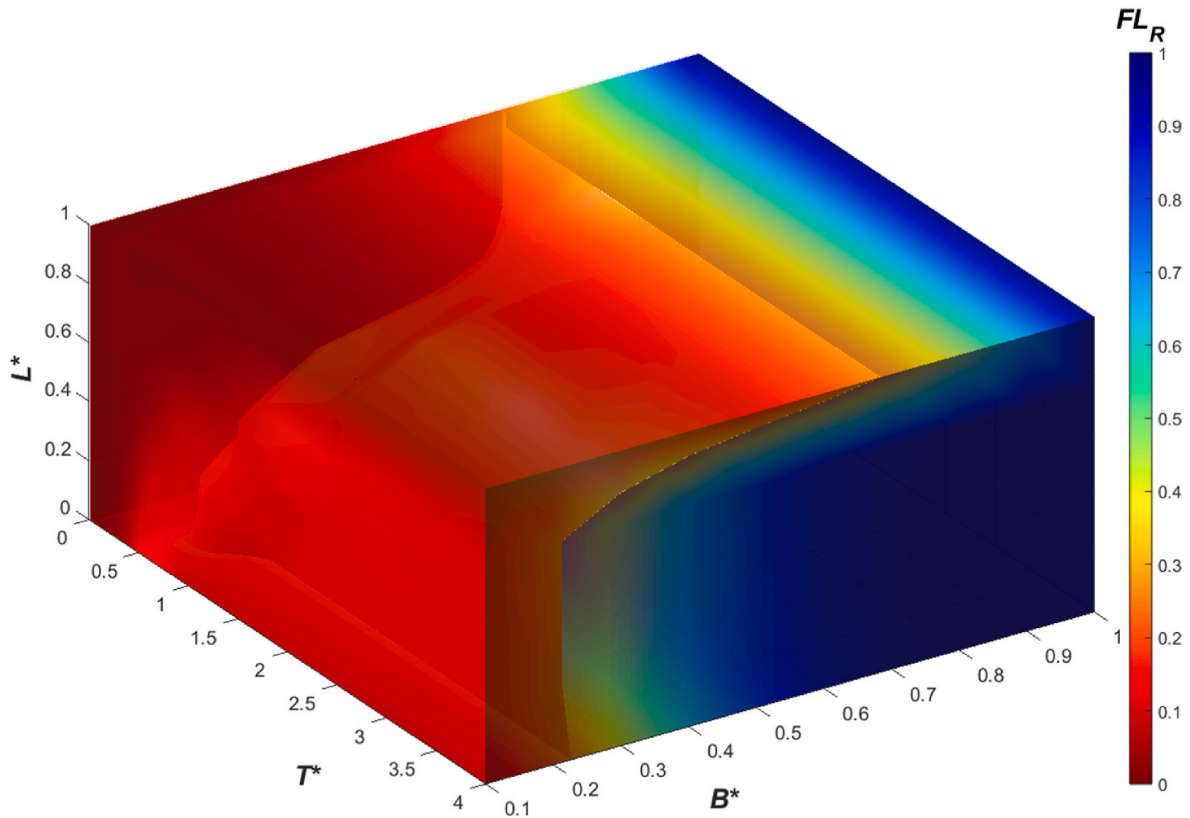


Fig. 9. Relative fatigue life ( $FL_R$ ) for various dimensionless length ratios ( $L^*$ ,  $B^*$ , and  $T^*$ ).

- If it is assumed that the case of the “long-duration pulses”, the individual waves are superimposed into one big pulse wave. When the pulse duration is long enough ( $T^* < 0.01$ ), all the wave reflections and incident waves merge into one big pulse wave, and the magnitude of the pulse reaches its maximum. In this case, the magnitude of the pulse is only dependent on  $B^*$ .

Normalized analysis with pressure damping can be analysed in a similar approach. It is not discussed in this analytical analysis section for brevity but will be considered in the numerical simulation discussed later.

## 6. Discussion

The findings in this research are potentially affected by additional factors which have not been considered in this paper. Firstly, the presented study only considers an infinitely long pipeline system without considering wave reflections from other components (e.g., branch, reservoir and etc) in the water distribution system. Secondly, fatigue life is also affected by other factors, such as inherent defects on the wall surface or the presence of external constraints. The implications are briefly discussed as follows.

### 6.1. Network complexity in WDSs

In real water distribution systems, reflections will be caused by network connections such as branches, multiway junctions, or dead-ends. These network connections may change the amplitude of the transient waves. In some cases, the amplitude can be increased. An example is presented in Fig. 10(a), where a short section of plastic pipe is connected to the dead-end of the pipeline system. Such pipeline configuration is often observed in household pipelines that are connected to the water main. The transient wave may be superimposed in

this pipeline configuration, particularly for pulse waves [17,23]. However, the network connections may also decrease the amplitude of the transient waves. For example, as shown in Fig. 10(b), where a short section of plastic pipe is installed between two metallic water mains. The hydraulic impedance in the metallic mains is typically higher than that of the plastic pipe. As a result, the reflected waves from the metallic mains have an opposite sign to the incident wave. In this case, some of the pressure waves may be cancelled out by the reflected waves [47].

### 6.2. Effect of pipe defects

In real water distribution systems, defects on the plastic pipe wall are not avoidable due to degradation, improper installation or manufacturing defects [48]. Such defects on the pipe wall can cause stress concentration on the micro-voids. The lifetime of the plastic pipe with defects can be normally predicted by fracture mechanics under static loading [33,35]. If defects, such as small cracks, exist on the wall of the plastic pipe in an M-P-M system, internal stress in the pipeline can be concentrated on the inherent defects which leads to small crack growth (SCG) and failure [49]. Failure mechanism of SCG can be described by a continuous formation and breakdown of crazes from initial crack tips [50]. As a results, the fatigue life is expected to be further reduced.

SCG kinetics of plastic pipe have been investigated by tools of the linear elastic fracture mechanics (LEFM) under static or cyclic loading condition [33–35,50]. With the knowledge of the crack kinetics of pipe material, LEFM provides lifetime prediction of complex structures [50]. LEFM methods have been used to predict lifetime of PE pipes under static [33] and cyclic [34] loading conditions. When inherent defects are presented on the plastic pipe surface, M-P-M system can also accelerate SCG and decrease expected fatigue lifetime [33–35,50]. With the knowledge of the crack kinetics of pipe material, LEFM provides lifetime prediction of complex structures [50]. LEFM methods have been used to

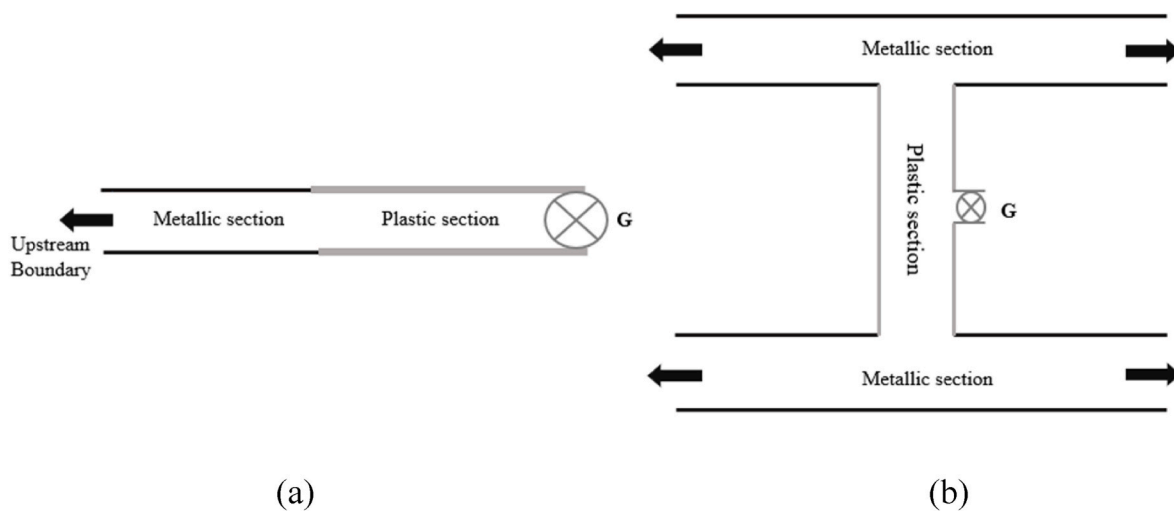


Fig. 10. Examples of network complexity in WDSs: (a) Plastic section at the end of the pipe with valve; (b) Plastic pipe connecting two metallic pipes.

predict lifetime of PE pipes under static [33] and cyclic [34] loading conditions. When inherent defects are presented on the plastic pipe surface, M-P-M system can also accelerate SCG and decrease expected fatigue lifetime.

## 7. Conclusion

This research has demonstrated that the impedance mismatch in metallic-plastic-metallic (M-P-M) pipe systems can significantly accelerate the fatigue of the plastic section when compared to the fully plastic pipeline configuration. When the system is experiencing hydraulic transient events, the multiple wave reflections due to impedance mismatch cause additional stress loadings to the plastic section. Moreover, the multiple wave reflections and the incident wave may overlap with each other, and merge into a larger pressure perturbation (larger stress loading). This can impose more fatigue damage to the pipe than having the individual waves in sequence.

The wave propagation in the M-P-M system has been investigated analytically. A general form of the pressure response for the M-P-M pipeline system has been derived to analyse the pressure responses in any M-P-M systems without the implementation of numerical simulations.

Fatigue analysis has been conducted using the derived pressure responses and a stress-life fatigue model. It is shown that the relative fatigue life (relative to the fully plastic configuration) is determined by three dimensionless parameters of the M-P-M pipeline system: normalized length ( $L^*$ ), normalized pulse duration ( $T^*$ ) and impedance ratio ( $B^*$ ). The results show that the relative fatigue life can be reduced significantly depending on the impedance ratio and the pulse wave duration.

Numerical case studies have been conducted on an M-P-M configuration with PVC and Ductile Iron (DI) pipe sections. Pressure responses to incident pulse pressure waves with various pulse durations and various sizes have been simulated by MOC and the relative fatigue life calculated using the fatigue model. The results from the numerical simulations are consistent with the results from the analytical analysis.

The damping of pressure waves due to energy losses reduced the magnitude of pressure waves. When energy loss is considered, it will result in less reduction of the relative fatigue life when compared to the results from the lossless scenario. However, the difference is generally insignificant comparing to the overall reduction in relative fatigue life. The impact decreases with the decrease in length of the plastic section in the M-P-M system.

Overall, the findings of this study suggest that the impedance mismatch between two adjacent pipe sections can have a negative

impact on the plastic pipe fatigue lifetime. It is necessary to consider this impact in pipe system design, especially when the system is subjected to repeated hydraulic transient events.

This study is limited to numerical and analytical analysis. Future work can include experimental validation of the fatigue lifetime, 3-dimensional studies of the boundary reflections, and quantify the impact of pipe wall defects.

## Credit author statement

Ji-Sung Lee: Software, Formal analysis, Investigation, Writing – original draft Wei Zeng: Writing – review & editing, Data curation, Investigation Martin Lambert: Writing – review & editing, Supervision, Funding acquisition Timothy Hilditch: Writing – review & editing, Supervision Jinzhe Gong: Conceptualization, Writing – review & editing, Supervision, Funding acquisition, Methodology.

## Declaration of competing interest

The authors declare that they have no known competing financial interests or personal relationships that could have appeared to influence the work reported in this paper.

## Data availability

Data will be made available on request.

## Acknowledgement

The research presented in the paper has been supported by the Australian Research Council through the Linkage Project Scheme (LP180100569).

## References

- [1] K. Pietrucha-Urbaniak, Failure analysis and assessment on the exemplary water supply network, *Eng. Fail. Anal.* 57 (2015) 137–142.
- [2] S.-G. Kim, K.-B. Lee, K.-Y. Kim, Water hammer in the pump-rising pipeline system with an air chamber, *J. Hydrodyn.* 26 (6) (2014) 960–964.
- [3] Y.-F. Liu, J.-X. Zhou, Q. Guo, A.-L. Shen, J. Zhang, 3-D CFD simulation of transients in multiple pump system with some pumps being stopped, *J. Hydrodyn.* 33 (3) (2021) 583–592.
- [4] O. Awe, S. Okolie, O. Fayomi, Analysis and optimization of water distribution systems: a case study of Kurudu post service housing estate, Abuja, Nigeria, *Results in Engineering* 5 (2020), 100100.
- [5] X.-L. Guo, K.-L. Yang, F.-T. Li, T. Wang, Analysis of first transient pressure oscillation for leak detection in a single pipeline, *J. Hydrodyn.* 24 (3) (2012) 363–370.

- [6] A. Firouzi, W. Yang, W. Shi, C.-Q. Li, Failure of corrosion affected buried cast iron pipes subject to water hammer, *Eng. Fail. Anal.* 120 (2021), 104993.
- [7] M. Bouaziz, M. Guidara, C. Schmitt, E. Hadj-Taieb, Z. Azari, Water hammer effects on a gray cast iron water network after adding pumps, *Eng. Fail. Anal.* 44 (2014) 1–16.
- [8] Y. Mou, Z. Lian, P. Sang, H. Yu, Q. Zhang, R. Li, Study on water hammer effect on defective tubing failure in high pressure deep gas well, *Eng. Fail. Anal.* 106 (2019), 104154.
- [9] M.L. Stephens, J. Gong, A. Marchi, M.F. Lambert, A.R. Simpson, Transient pressure data collection and characterisation in identifying options for reducing pipe fatigue, in: 13th Hydraulics in Water Engineering, Engineers Australia, Sydney, NSW, 2017.
- [10] Y. Huang, F. Zheng, H.-F. Duan, Q. Zhang, Multi-objective optimal design of water distribution networks accounting for transient impacts, *Water Resour. Manag.* 34 (4) (2020) 1517–1534.
- [11] A. Haghighi, Analysis of transient flow caused by fluctuating consumptions in pipe networks: a many-objective genetic algorithm approach, *Water Resour. Manag.* 29 (7) (2015) 2233–2248, <https://doi.org/10.1007/s11269-015-0938-6>.
- [12] S. Rathnayaka, B. Shannon, P. Rajeev, J. Kodikara, Monitoring of pressure transients in water supply networks, *Water Resour. Manag.* 30 (2) (2016) 471–485, <https://doi.org/10.1007/s11269-015-1172-y>.
- [13] I. Hobbs, M. Anda, P.A. Bahri, Estimating peak water demand: literature review of current standing and research challenges, *Results in Engineering* 4 (2019), 100055.
- [14] M. Stephens, J. Gong, C. Zhang, A. Marchi, L. Dix, M.F. Lambert, Leak-before-break main failure prevention for water distribution pipes using acoustic smart water technologies: case study in adelaide, *J. Water Resour. Plann. Manag.* 146 (10) (2020), 05020020, [https://doi.org/10.1061/\(ASCE\)WR.1943-5452.0001266](https://doi.org/10.1061/(ASCE)WR.1943-5452.0001266).
- [15] G. Pezzinga, P. Scandura, Unsteady flow in installations with polymeric additional pipe, *J. Hydraul. Eng.* 121 (11) (1995) 802–811.
- [16] G. Pezzinga, Unsteady flow in hydraulic networks with polymeric additional pipe, *J. Hydraul. Eng.* 128 (2) (2002) 238–244.
- [17] J. Gong, M.L. Stephens, M.F. Lambert, A.C. Zecchin, A.R. Simpson, Pressure surge suppression using a metallic-plastic-metallic pipe configuration, *J. Hydraul. Eng.* 144 (6) (2018), [https://doi.org/10.1061/\(asce\)hy.1943-7900.0001468](https://doi.org/10.1061/(asce)hy.1943-7900.0001468).
- [18] M. Kubrak, A. Kodura, A. Malesińska, K. Urbanowicz, Water hammer in steel-plastic pipes connected in series, *Water* 14 (19) (2022) 3107.
- [19] N. Bettaieb, M.A. Guidara, E. Haj Taieb, Impact of metallic-plastic pipe configurations on transient pressure response in branched WDN, *Int. J. Pres. Ves. Pip.* 188 (2020), <https://doi.org/10.1016/j.ijpvp.2020.104204>.
- [20] L. Hadj Taieb, N. Bettaieb, M.A. Guidara, S. Elaoud, E. Haj Taieb, Effect of integrating polymeric pipes on the pressure evolution and failure assessment in cast iron branched networks, *Eng. Fract. Mech.* 235 (2020), <https://doi.org/10.1016/j.engfracmech.2020.107158>.
- [21] A. Triki, M.A. Chaker, Compound technique -based inline design strategy for water-hammer control in steel pressurized-piping systems, *Int. J. Pres. Ves. Pip.* 169 (2019) 188–203, <https://doi.org/10.1016/j.ijpvp.2018.12.001>.
- [22] M.H. Chaudhry, *Applied Hydraulic Transients*, third ed., Springer, New York, 2014.
- [23] J. Bohorquez, M.F. Lambert, A.R. Simpson, Identifying head accumulation due to transient wave superposition in pipelines, *J. Hydraul. Eng.* 146 (1) (2020), [https://doi.org/10.1061/\(asce\)hy.1943-7900.0001631](https://doi.org/10.1061/(asce)hy.1943-7900.0001631).
- [24] J.-S. Lee, J. Gong, W. Zeng, M.F. Lambert, Fatigue analysis of metallic-plastic-metallic pipeline systems: a numerical case study, in: ACAM10: 10th Australasian Congress on Applied Mechanics, Engineers Australia, Adelaide, Australia, 2021, pp. 714–725.
- [25] S. Folkman, R. Bishop, A simple design procedure for PVC pipe to account for cyclic pressure loading, in: Proceedings of the 18th Plastic Pipes Conference, 2016 (Berlin).
- [26] J.D. Jeffrey, A. Moser, S.L. Folkman, New design guidelines for fatigue failure in PVC pipe, in: *Plastics Pipes XII Conference Proceedings*, 2003, Milan, Italy.
- [27] S. Joseph, P. Leever, Failure mechanics of uPVC cyclically pressurized water pipelines, *J. Mater. Sci.* 20 (1) (1985) 237–245.
- [28] A.J. Whittle, A. Teo, Resistance of PVC-U and PVC-M to cyclic fatigue, *Plast., Rubber Compos.* 34 (1) (2005) 40–46, <https://doi.org/10.1179/174328905X29776>.
- [29] F. Majid, M. Elghorba, HDPE pipes failure analysis and damage modeling, *Eng. Fail. Anal.* 71 (2017) 157–165, <https://doi.org/10.1016/j.engfailanal.2016.10.002>.
- [30] H.W. Vinson, Response of PVC pipe to large, repetitive pressure surges, in: *Underground Plastic Pipe*, ASCE, 1981.
- [31] S. Folkman, J. Parvez, PVC pipe cyclic design method, in: *Pipelines 2020*, American Society of Civil Engineers, 2020.
- [32] S. Burn, P. Davis, T. Schiller, Long-term Performance Prediction for PVC Pipes, 2005.
- [33] P. Hutař, L. Náhlík, L. Šestáková, M. Ševčík, Z. Kněs, E. Nezbedová, A fracture mechanics assessment of surface cracks existing in protective layers of multi-layer composite pipes, *Compos. Struct.* 92 (5) (2010) 1120–1125, <https://doi.org/10.1016/j.compstruct.2009.10.004>.
- [34] A. Frank, F.J. Arbeiter, I.J. Berger, P. Hutař, L. Náhlík, G. Pinter, Fracture mechanics lifetime prediction of polyethylene pipes, *J. Pipeline Syst. Eng. Pract.* 10 (1) (2019), 04018030.
- [35] A. Frank, G. Pinter, R.W. Lang, Prediction of the remaining lifetime of polyethylene pipes after up to 30 years in use, *Polym. Test.* 28 (7) (2009) 737–745, <https://doi.org/10.1016/j.polymertesting.2009.06.004>.
- [36] Awwa, ANSI/AWWA C900-07 (Revision of ANSI/AWWA C900-97), AWWA Standard Polyvinyl Chloride (PVC) Pressure Pipe and Fabricated Fittings, American Water Works Association, 2007.
- [37] R.T. Hucks, Design of PVC water-distribution pipe, *Civ. Eng.* 42 (6) (1972) 70–73.
- [38] J.A. Bowman, The Fatigue Response of Polyvinyl Chloride and Polyethylene Pipe Systems, ASTM International, 1990.
- [39] E.B. Wylie, V.L. Streeter, *Fluid Transients in Systems*, Prentice Hall Inc, Englewood Cliffs, New Jersey, USA, 1993, p. 463.
- [40] E.B. Wylie, The microcomputer and pipeline transients, *J. Hydraul. Eng.* 109 (12) (1983) 1723–1739.
- [41] A. Keramat, A.S. Tijsseling, Q. Hou, A. Ahmadi, Fluid-structure interaction with pipe-wall viscoelasticity during water hammer, *J. Fluid Struct.* 28 (2012) 434–455, <https://doi.org/10.1016/j.jfluidstruct.2011.11.001>.
- [42] D. Covas, I. Stoianov, J.F. Mano, H. Ramos, N. Graham, C. Maksimovic, The dynamic effect of pipe-wall viscoelasticity in hydraulic transients. Part I - experimental analysis and creep characterization, *J. Hydraul. Res.* 42 (5) (2004) 516–530.
- [43] D. Covas, I. Stoianov, J. Mano, H. Ramos, N. Graham, C. Maksimovic, The dynamic effect of pipe-wall viscoelasticity in hydraulic transients. Part II - model development, calibration and verification, *J. Hydraul. Res.* 43 (1) (2005) 56–70.
- [44] J. Gong, Y.-I. Kim, H. Fandrich, M.F. Lambert, A.R. Simpson, A.C. Zecchin, Field study on pipeline parameter identification using fluid transient waves with time-domain analysis, in: 12th International Conference on Pressure Surges, Ireland BHR Group, Dublin, 2015.
- [45] W. Zeng, A.C. Zecchin, J. Gong, M.F. Lambert, A.R. Simpson, B.S. Cazzolato, Inverse wave reflectometry method for hydraulic transient-based pipeline condition assessment, *J. Hydraul. Eng.* 146 (8) (2020), [https://doi.org/10.1061/\(ASCE\)HY.1943-7900.0001785](https://doi.org/10.1061/(ASCE)HY.1943-7900.0001785).
- [46] P.P.I. Ppi, *Handbook of Polyethylene Pipe*, CLVR Company, 2012.
- [47] J. Leckner, *Theory of Reflection: Reflection and Transmission of Electromagnetic, Particle and Acoustic Waves*, John Wiley & Sons, New York, 1973.
- [48] H. Rezaei, B. Ryan, I. Stoianov, Pipe failure analysis and impact of dynamic hydraulic conditions in water supply networks, *Procedia Eng.* 119 (2015) 253–262, <https://doi.org/10.1016/j.proeng.2015.08.883>.
- [49] K. Oliphant, M. Conrad, W. Bryce, Fatigue of Plastic Water Pipe: A Technical Review with Recommendations for PE4710 Pipe Design Fatigue, *Pipelines 2012: Innovations in Design, Construction, Operations, and Maintenance, Doing More with Less*, 2012, pp. 38–60.
- [50] A. Frank, P. Hutař, G. Pinter, Numerical assessment of PE 80 and PE 100 pipe lifetime based on Paris-Erdogan equation, in: *Macromolecular Symposia*, Wiley Online Library, 2012.